

Symmetric quadratic tetration interpolation using forward and backward operation combination

Chapkit Charmsamorn, Suphongs Khetkeeree

Physics Department, Faculty of Science, Mahanakorn University of Technology, Bangkok, Thailand

Article Info

Article history:

Received Apr 29, 2021

Revised Sep 16, 2021

Accepted Oct 10, 2021

Keywords:

Curve fitting

Hyper-operation

Hyperpower

Signal reconstruction

Super exponentiation

ABSTRACT

The existed interpolation method, based on the second-order tetration polynomial, has the asymmetric property. The interpolation results, for each considering region, give individual characteristics. Although the interpolation performance has been better than the conventional methods, the symmetric property for signal interpolation is also necessary. In this paper, we propose the symmetric interpolation formulas derived from the second-order tetration polynomial. The combination of the forward and backward operations was employed to construct two types of the symmetric interpolation. Several resolutions of the fundamental signals were used to evaluate the signal reconstruction performance. The results show that the proposed interpolations can be used to reconstruct the fundamental signal and its peak signal to noise ratio (PSNR) is superior to the conventional interpolation methods, except the cubic spline interpolation for the sine wave signal. However, the visual results show that it has a small difference. Moreover, our proposed interpolations converge to the steady-state faster than the cubic spline interpolation. In addition, the option number increasing will reinforce their sensitivity.

This is an open access article under the [CC BY-SA](https://creativecommons.org/licenses/by-sa/4.0/) license.



Corresponding Author:

Suphongs Khetkeeree

Physics Department, Mahanakorn University of Technology

140 Cheum-Sampan Road, Nongchok, Bangkok 10530, Thailand

Email: suphongs@mutacth.com

1. INTRODUCTION

Recently, the technology based on digital information is rapidly growing up. It can change the human lifestyle. Some information can be easily learned and applied to the real world. However, all data cannot be kept in digital form due to a lot of limitations, such as storage size, sampling technique, or communication constraints. In order to obtain the unknown data from its related known data, interpolation is an important method. It has been widely applied in several applications, i.e., signal reconstruction [1]–[9], signal and image denoising [10]–[12], medical image processing [13]–[18], image resizing [19]–[28], image classification [29], image compression [30], image enhancement [31], change detection [32], video processing [33], and more [34], [35]. The interpolation is used to generate the new data points from the discrete set of known data points in case of its position is within the range of known data. The simplest method is the nearest neighbor interpolation employed the data value of the nearest location to estimate the new data points. This method is the same fashions of the piecewise constant function. It is an advantage for the lowest computing time but lacks performance for other situations. These problems can be solved by substitute the piecewise constant function with the higher-order polynomial, i.e., the linear interpolation [36] or the cubic interpolation. The linear interpolation gives the computing time lower than the cubic interpolation, but the reconstruction performance in smoothing signal is poor. We tried to apply the tetration

mathematics, which is the next mathematical operation after exponentiation in our previous work, for modeling the alternative formulas for signal interpolation [2] as:

- Tetration polynomial: the tetration is one of the mathematical operations located after exponentiation but before pentation. It was firstly proposed by Goodstein [37] in 1947. He used the notation ${}^n x$ instead of the application $n - 1$ time of x , that is:

$${}^n x = \overbrace{x^{x^{\cdot^{\cdot^{\cdot^x}}}}}^n, \quad (1)$$

however, there are many notations for the tetration, i.e., $x \uparrow n$ for [38] and uxp_x^n for [39]. Moreover, it also can be called for a different name such as superexponentiation [40], hyperpower [41]. This mathematical operator was applied in the problem of compacting Church numerals [42], and our previous work [2]. The form of the traditional polynomial function was used to model the tetration polynomial function. It is the additional series that each term is the multiplication of the arbitrary constant (a_n) and any order tetration. We can write in the summation form as (2):

$$f(x) = \sum_{n=0}^m a_n ({}^n x), m \in N \quad (2)$$

- Existed tetration interpolation: the simple quadratic tetration polynomial was considered in our previous work [2], written as (3):

$$f_F(x) = a_0 + a_1 \cdot x + a_2 \cdot {}^2 x \quad (3)$$

If we know the data of any considering signal as (x_1, y_1) , (x_2, y_2) , and (x_3, y_3) , therefore we can construct the system of equation for these points as (4):

$$\begin{bmatrix} 1 & x_1 & {}^2 x_1 \\ 1 & x_2 & {}^2 x_2 \\ 1 & x_3 & {}^2 x_3 \end{bmatrix} \begin{bmatrix} a_0 \\ a_1 \\ a_2 \end{bmatrix} = \begin{bmatrix} y_1 \\ y_2 \\ y_3 \end{bmatrix} \quad (4)$$

In the tasks of discrete signal processing, we can define x_1, x_2 and x_3 as the non-negative integer numbers. Thus, the solution of above system of equation can be found. Several techniques can be used for calculating the parameters a_0, a_1 , and a_2 . In this paper, we employed the Cramer's rule for determining solution of (4) as (5).

$$\begin{aligned} a_0 &= \frac{y_1({}^2 x_3 x_2 - {}^2 x_2 x_3) + y_2({}^2 x_1 x_3 - {}^2 x_3 x_1) + y_3({}^2 x_2 x_1 - {}^2 x_1 x_2)}{({}^2 x_3 x_2 - {}^2 x_2 x_3) + ({}^2 x_1 x_3 - {}^2 x_3 x_1) + ({}^2 x_2 x_1 - {}^2 x_1 x_2)} \\ a_1 &= \frac{y_1({}^2 x_2 - {}^2 x_3) + y_2({}^2 x_3 - {}^2 x_1) + y_3({}^2 x_1 - {}^2 x_2)}{({}^2 x_3 x_2 - {}^2 x_2 x_3) + ({}^2 x_1 x_3 - {}^2 x_3 x_1) + ({}^2 x_2 x_1 - {}^2 x_1 x_2)} \\ a_2 &= \frac{y_1(x_3 - x_2) + y_2(x_1 - x_3) + y_3(x_2 - x_1)}{({}^2 x_3 x_2 - {}^2 x_2 x_3) + ({}^2 x_1 x_3 - {}^2 x_3 x_1) + ({}^2 x_2 x_1 - {}^2 x_1 x_2)} \end{aligned} \quad (5)$$

- Forward and backward operations: The above interpolation formula (3) has the shift variant and asymmetric properties [2]. It gives an individual value for each domain range. For example, if we set the value of y_1, y_2 , and y_3 as any fixed real number and set x_1, x_2, x_3 are the non-negative integer number with arranged order. The interpolation results can be shown as Figure 1(a). The word *Option* means as the set of sampling step position. Each option can be defined as $x_1 = 0, x_2 = 1, x_3 = 2$ for Option 1; $x_1 = 1, x_2 = 2, x_3 = 3$ for option 2; $x_1 = 2, x_2 = 3, x_3 = 4$ for option 3, and so on. The interpolation results were compared with the curve fitting of the quadratic polynomial. The simulation results show that the interpolated curve of the quadratic tetration polynomial for each option changes with asymmetry. It gives a high sensitivity on the right and provides a low sensitivity on the left. The effect of the option is for reinforcement of the response varied on the number of the option. The formula (3) will be called forward operation because it was operated from left to right of considered points. In the other hand, if the positions are operated from right to left, we called backward operation, which the interpolation results can be shown as Figure 1(b), and can be expressed as (6):

$$f_B(x) = a_0 + a_1 \cdot (x_0 - x) + a_2 \cdot {}^2(x_0 - x) \quad (6)$$

where $a_0, a_1,$ and a_2 are the parameters, which can be calculated from (5), and x_0 is a backward constant being equal two times of the option number.

Following the above methods, we found that it can be applied to reconstruct the fundamental degraded signals with many specific properties, i.e., shift variant and asymmetric properties. However, the symmetric property is also necessary for several applications. In this paper, the symmetric signal interpolation based on a quadratic tetration polynomial was proposed. The rest of this paper can be organized as follows. The methods for constructing the interpolation formulas, both asymmetric and symmetric formulas, are presented and described in section 2. Then, the research method is illustrated in section 3. The experimental results of the fundamental signal are demonstrated and discussed in section 4. Finally, we give the concluding remarks in section 5.

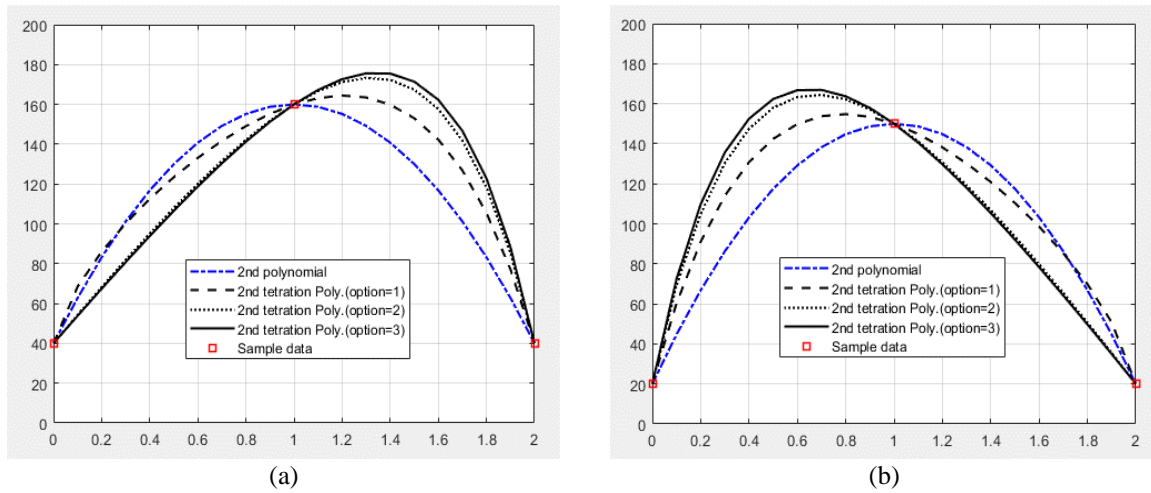


Figure 1. Curve fitting of the quadratic tetration polynomial of option 1, 2, and 3, compared with The normal quadratic polynomial for (a) forward operation and (b) backward operation

2. PROPOSED METHOD

2.1. Asymmetric tetration interpolation

The option 1 was selected to demonstrate our approach techniques. That is, the value of $x_1, x_2,$ and x_3 are 0, 1 and 2, respectively. In this option, the (5) can be reduced in the short form as $a_0 = \frac{1}{3}(2y_1 + 2y_2 - y_3), a_1 = \frac{1}{3}(-y_1 + y_2),$ and $a_2 = \frac{1}{3}(y_1 - 2y_2 + y_3).$ Therefore, we can build the Forward interpolation formula by substitute of the constant a_0, a_1 and a_2 into (3). That is:

$$y_{Forward} = A_1y_1 + A_2y_2 + A_3y_3 \tag{7}$$

where

$$A_1 = \frac{1}{3}(2 - 3x + {}^2x)$$

$$A_2 = \frac{1}{3}(2 + 3x - 2({}^2x)) \text{ , } x \in (0,2)$$

$$A_3 = \frac{1}{3}(-1 + {}^2x).$$

Likewise, the backward interpolation formula can be expressed as (8):

$$y_{Backward} = B_1y_1 + B_2y_2 + B_3y_3 \tag{8}$$

where

$$B_1 = \frac{1}{3}(-1 + {}^2(x_0 - x))$$

$$B_2 = \frac{1}{3}(2 + 3(x_0 - x) - 2 \cdot {}^2(x_0 - x)) , x \in (0,2) \text{ and } x_0 = 2.$$

$$B_3 = \frac{1}{3}(2 - 3(x_0 - x) + {}^2(x_0 - x))$$

The interpolation results on the left side (0, 1] and the right side [1, 2) give the different results (asymmetric property). We can demonstrate four different techniques of asymmetric interpolation as follows. Firstly, the interpolation result on the left side of the Forward operation is considered. It was called forward-left (F-L) tetration interpolation. Also, if the interpolation result on the right side of the forward operation is considered, it will be called forward-right (F-R) tetration interpolation. Some behavior of such techniques for square wave signal reconstruction can be demonstrated in Figure 2(a) and Figure 2(b). In the same way, the backward-left (B-L) tetration interpolation and the backward-right (B-R) tetration interpolation will employ the interpolation result of the backward operation on the left and right sides, respectively. Figure 3(a) and Figure 3(b) illustrates the reconstruction of the B-L and B-R tetration interpolations for the square wave signal case.

We can summarize the preliminary dominant results as follows. The F-R and B-L interpolation techniques give a higher edge overshoot than the F-L and B-R techniques. The edge overshoot does not appear in both terminal sides of the changing region that is different for the cubic spline interpolation. The edge overshoot of the same operation does not appear on the same location, but it gives a similar location when they have the same considered side. For example, the F-L and B-L are the same edge overshoot location. Likewise, the F-R and B-R have the same location of the edge overshoot.

2.2. Symmetric tetration interpolation

In order to correct the asymmetric behavior, the arithmetic mean of the combination of the F-L interpolation and B-R interpolation is used to formulate the symmetric interpolation formulas. Because of the behavior of both F-L interpolation and B-R interpolation, it is low sensitivity with the high-frequency components or the changing region as shown in Figure 2(a) and Figure 3(b). We will call this interpolation as low sensitivity tetration (LOST) interpolation. This formula can be simply expressed as follows, LOST interpolation;

$$y_{\text{LOST}} = \alpha_1 y_{i-1} + \alpha_2 y_i + \alpha_3 y_{i+1} + \alpha_4 y_{i+2} \quad (9)$$

where

$$\alpha_1 = \frac{1}{6}(-1 + {}^2(1 - x))$$

$$\alpha_2 = \frac{1}{6}(7 - 6 \cdot x + {}^2x - 2 \cdot {}^2(1 - x)), x \in (0,1)$$

$$\alpha_3 = \frac{1}{6}(1 + 6 \cdot x - 2 \cdot {}^2x + {}^2(1 - x))$$

$$\alpha_4 = \frac{1}{6}(-1 + {}^2x)$$

Likewise, the arithmetic mean of the combination of the F-R interpolation and B-L interpolation is used to formulate the high-sensitivity symmetric interpolation formula. This formula has the opposite behavior with the LOST interpolation because it was constructed from two high sensitivity formulas as shown in Figure 2(b) and Figure 3(a). Therefore, this formula will be called high sensitivity tetration (HIST) interpolation. Its formula can be expressed as follows. HIST interpolation;

$$y_{\text{HIST}} = \beta_1 y_{i-1} + \beta_2 y_i + \beta_3 y_{i+1} + \beta_4 y_{i+2} \quad (10)$$

where

$$\beta_1 = \frac{1}{6}(-1 - 3 \cdot x + {}^2(1 + x))$$

$$\beta_2 = \frac{1}{6}(4 + 3 \cdot x - 2 \cdot x^2(1 + x) + x^2(2 - x)), x \in (0,1)$$

$$\beta_3 = \frac{1}{6}(7 - 3 \cdot x + x^2(1 + x) - 2 \cdot x^2(2 - x))$$

$$\beta_4 = \frac{1}{6}(-4 + 3 \cdot x + x^2(2 - x))$$

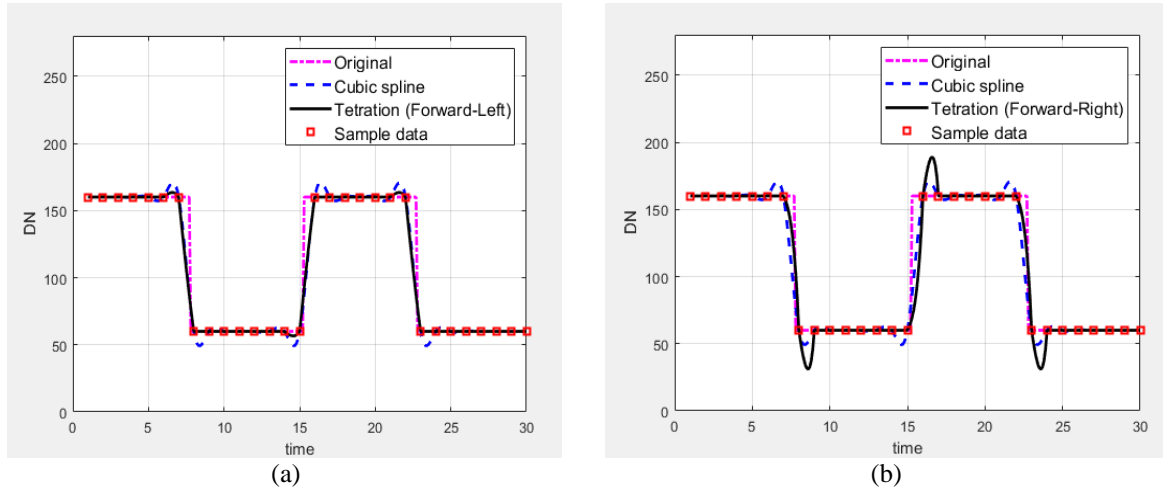


Figure 2. Comparison of the square wave interpolation result with (a) F-L tetration interpolation and (b) F-R tetration interpolation

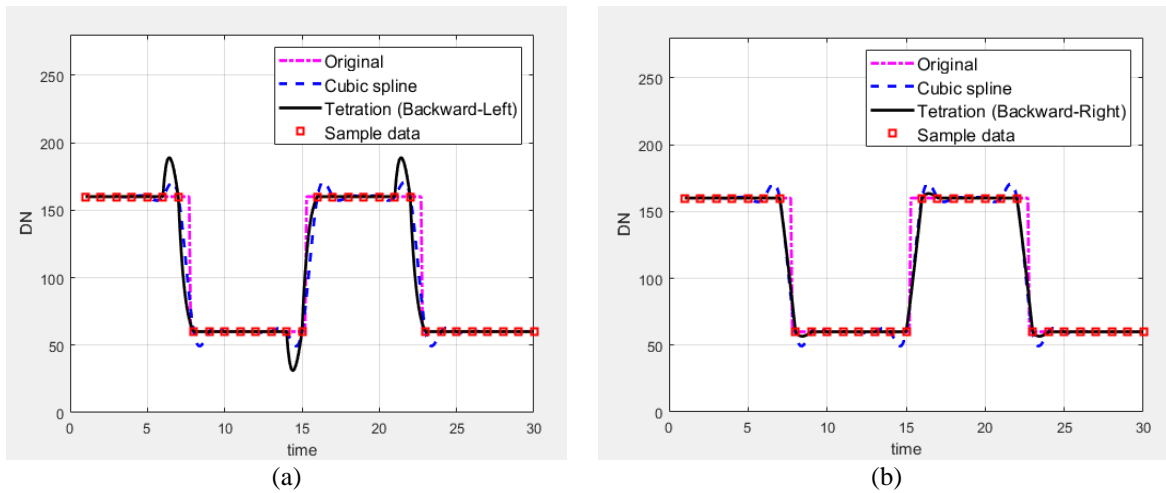


Figure 3. Comparison of the square wave interpolation result with (a) B-L tetration interpolation and (b) B-R tetration interpolation

3. RESEARCH METHOD

In order to evaluate our proposed method, the MATLAB program version R2018a was employed to implement the experimental results. Three fundamental synthetic signals i.e., square wave signal, a saw-tooth wave signal, and sine wave signal with several sampling resolutions were simulated and applied. It was designed for observing the performance limitations. Two comparison types were demonstrated as the quality metric and visual results. For the metric results, the peak signal to noise ratio or (PSNR) was employed to indicate the reconstruction quality. Our proposed methods were compared with three conventional methods, i.e., nearest-neighbor interpolation, linear interpolation, and cubic-spline interpolation. For the vision results, both our methods were illustrated in graph plot form and were compared with the cubic spline interpolation.

4. SIMULATION RESULTS AND DISCUSSION

The experimental results were divided into two parts as follows. The fundamental synthetic signals were employed to test our method performance in the first part. After that, the behavior of the option was demonstrated for observing the trend of the experimental result in second part.

4.1. Fundamental synthetic signal testing

The synthetic square wave signals were generated with 5, 15, 25, 35, and 45 samples per period and then were applied to all comparison methods, including our methods. The quality metric results were illustrated in Table 1. We can see, the LOST interpolation gives the highest PSNR results for all resolutions. For the HIST interpolation, it gives the PSNR value lower than others, except the nearest-neighbor method. The vision results were shown in Figure 4. Our methods were plotted comparing with the original data and the cubic spline interpolation. The HIST interpolation gives the behavior similar to the cubic spline interpolation for the edge region, but it tilts out of the edge as shown in Figure 4(a) in the zoom image.

Moreover, the HIST gives a behavior similar to the linear interpolation when it is out of the edge area. This behavior may be from the tetration polynomial that also has the first order normal polynomial (linear term) and its combination techniques. The vision results of LOST interpolation, it was demonstrated in Figure 4(b). We can see, the edge ringing is lower than others. Moreover, it also has a similar property with the HIST interpolation of both the tilt characteristic and off-edge region behavior.

Table 1. The PSNR value versus the sampling resolutions for the square wave signal

Resolution (Samples/Period)	Nearest	Linear	Cubic	LOST	HIST
5	13.9	15.2	14.7	15.2	15.0
15	18.6	20.1	20.1	20.2	20.0
25	20.7	22.3	22.3	22.4	22.2
35	22.3	23.8	23.8	23.9	23.6
45	23.4	24.9	24.9	25.0	24.7

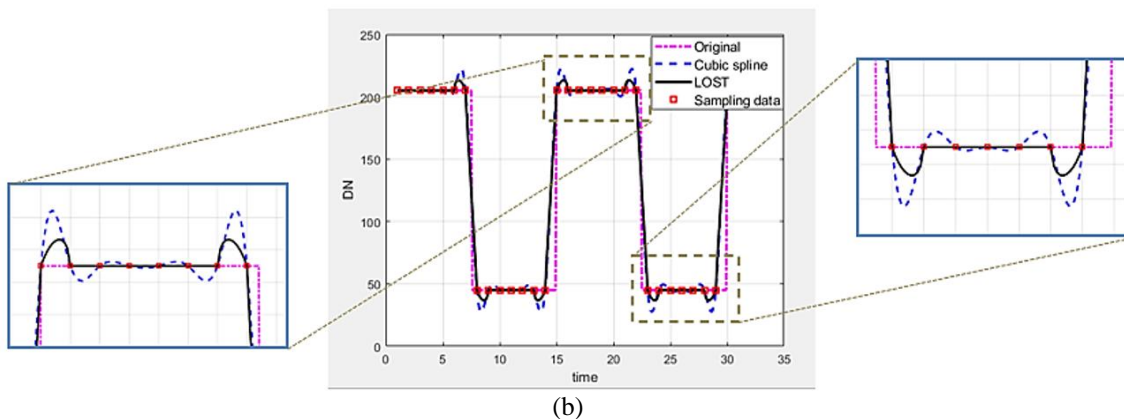
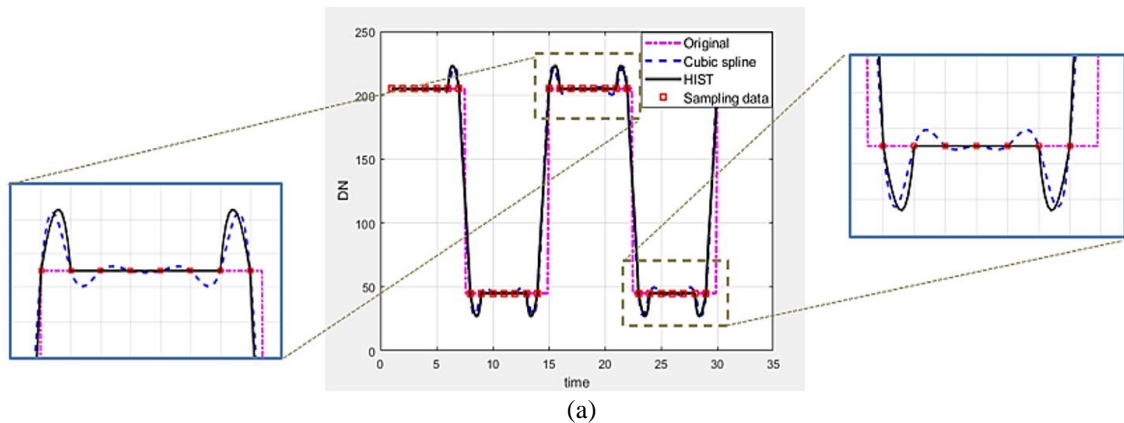


Figure 4. Comparison results between the cubic spline interpolation, (a) HIST interpolation and (b) LOST interpolation for the square wave signal

In the second experiment, we apply the saw-tooth wave signal to test our method performance. The visualization results of its behavior are demonstrated in Figures 5(a) and 5(b). For the quantitative comparison, the PSNR value of each method were shown in Table 2. The PSNR values of the LOST interpolation are also higher than others, following with the HIST interpolation. The zoom image in Figure 5(a) indicates that the HIST interpolation is also similar to the cubic spline interpolation, but it tilts out of the instantaneously changed edge. For this behavior, we may summarize as the tilt direction is opposite with the edge that has a higher slope. Moreover, the results also show that the linear property gives the converges to the steady-state faster than the cubic spline.

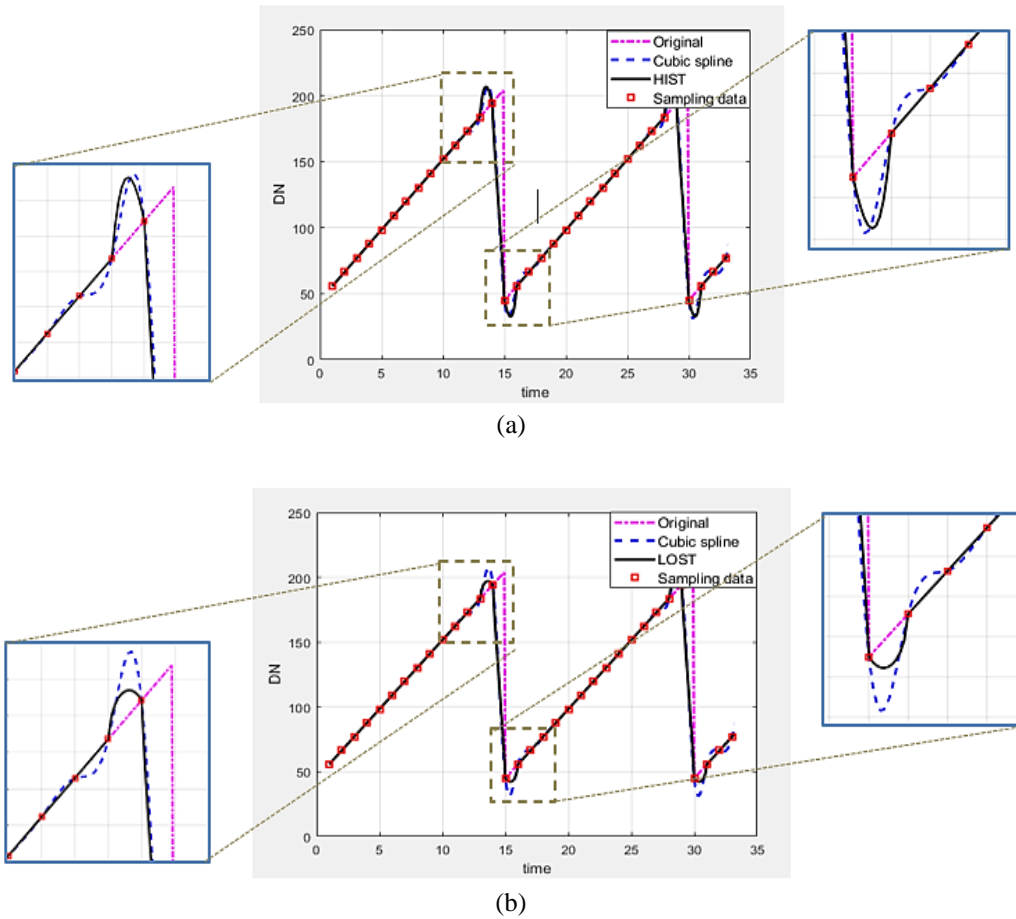


Figure 5. Comparison results between the cubic spline interpolation, (a) HIST interpolation and (b) LOST interpolation for the saw-tooth wave signal

Table 2. The PSNR values versus the sampling resolutions for the saw-tooth wave signal

Resolution (Samples/Period)	Nearest	Linear	Cubic	LOST	HIST
5	14.3	16.3	16.4	16.6	16.5
15	18.9	21.2	21.3	21.5	21.4
25	21.1	23.4	23.5	23.7	23.6
35	22.5	24.9	25.0	25.2	25.1
45	23.6	26.0	26.1	26.3	26.2

For the third experiment, we applied our interpolation methods to reconstruct the sine wave signal. The interpolated results can be illustrated in Table 3 for the quality metric results and in Figures 6(a) and 6(b) for the visual results. The results show that the cubic spline interpolation gives a higher PSNR than others, following by the LOST and HIST interpolation, respectively. For vision result of the HIST interpolation, it confirms that the tilt direction is dependent on the slope between both sides of the interpolation interval. The HIST interpolation is more sensitive with a rate of data change than the LOST interpolation. Although the

quality metric of the LOST interpolation looks more different than the cubic spline interpolation, the visual results are too close to cubic spline interpolation.

Table 3. The PSNR values versus the sampling resolutions for the sine wave signal

Resolution (Samples/Period)	Nearest	Linear	Cubic	LOST	HIST
5	21.9	30.2	48.2	37.9	38.8
15	31.4	49.0	92.6	62.3	51.7
25	35.8	57.8	114.0	72.1	60.1
35	38.7	63.7	127.1	78.2	65.9
45	40.9	68.1	136.4	82.7	70.2

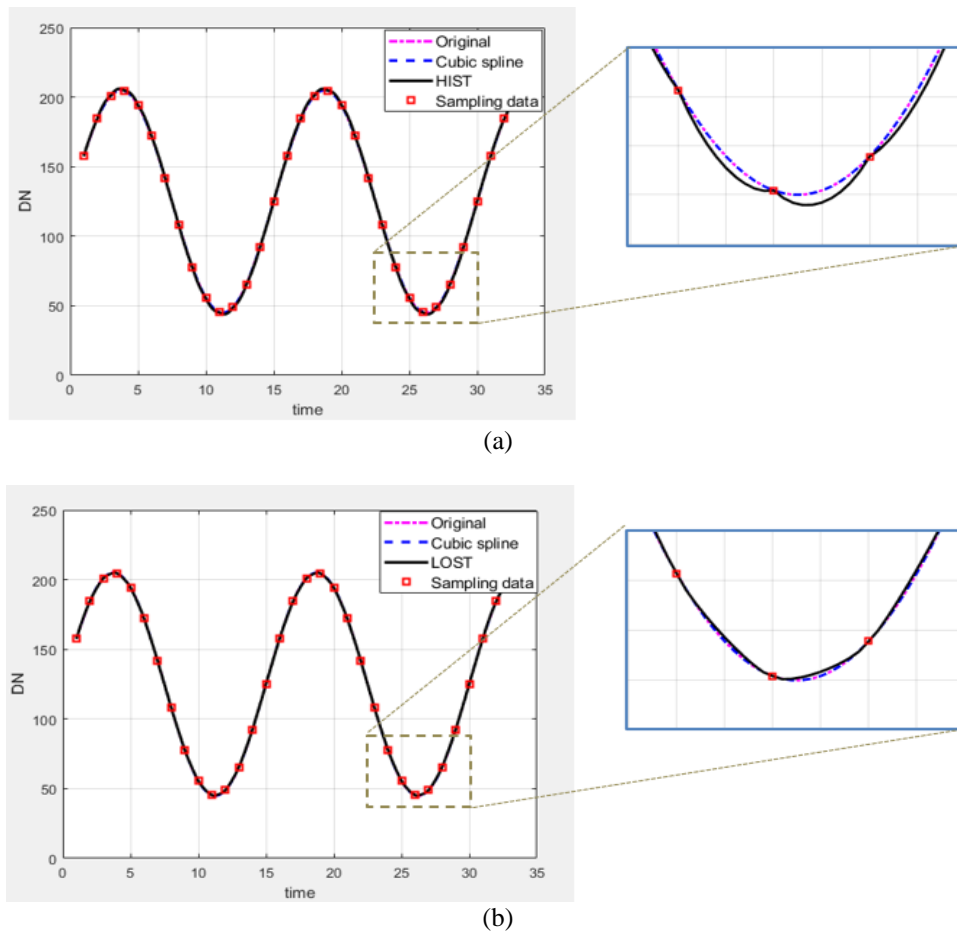


Figure 6. Comparison results between the cubic spline interpolation, (a) HIST interpolation and (b) LOST interpolation for the sine wave signal

4.2. Option behavior for symmetric tetration interpolation

In this subsection, the option 1, 2, and 3 were demonstrated compared with the original square wave signal and the result of the cubic spline interpolation for observing the behavior of our symmetric tetration interpolation. The vision results, both LOST and HIST interpolations, were illustrated in Figures 7(a) and 7(b). The results show that the edge overshoot of the LOST interpolation decrease when the option number is higher. Vice versa, the edge overshoot of HIST interpolation increases following the option number. For observing the quality metric with several sampling resolutions, the graph plot of the PSNR of the LOST, HIST, and cubic spline was presented in Figure 8. The LOST interpolation also gives a higher PSNR than others. The higher option number gives a better performance than the lower option number. However, the trend of performance result is a more similar value when the option number is much higher. Anyway, the higher option number gives the poor performance for the HIST interpolation. That means the option number increasing will provides higher sensitivity than the lower value.

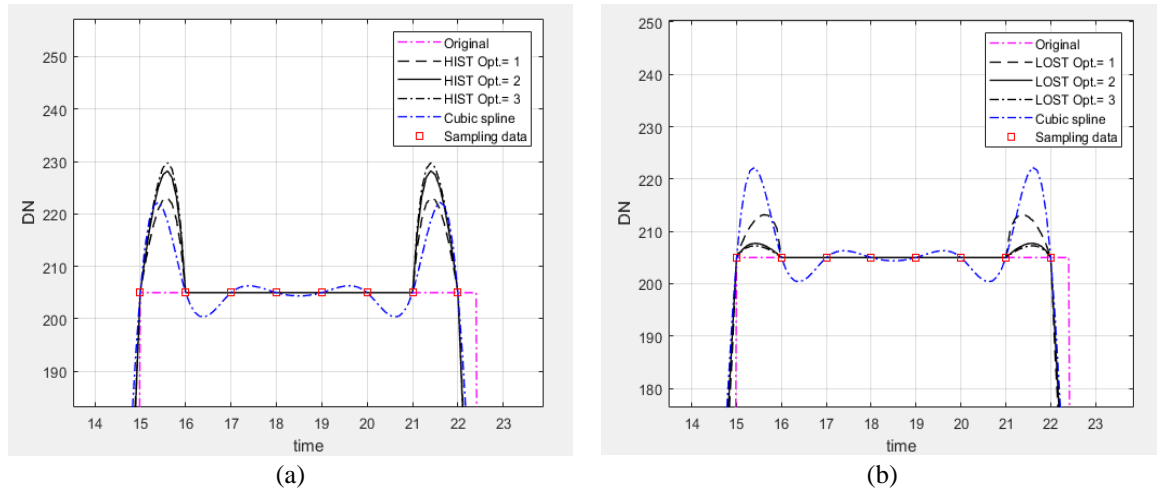


Figure 7. Comparison results between the cubic spline interpolation, (a) HIST interpolation and (b) LOST interpolation for the square wave signal with options 1, 2, and 3

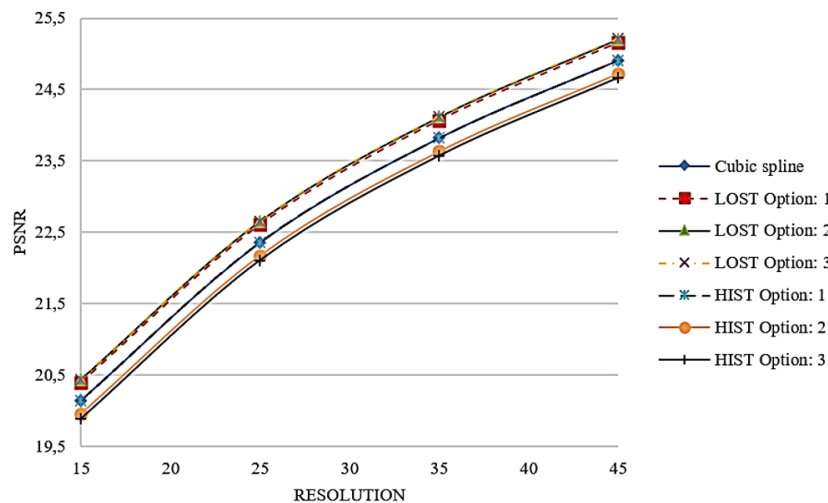


Figure 8. The PSNR comparison of HIST and LOST interpolations with options 1, 2, and 3 compared with the cubic spline interpolation for the square wave signal

5. CONCLUSION

In this paper, the symmetric tetration interpolation methods were proposed. It derived from the second-order (quadratic) tetration polynomial. Four types of asymmetric interpolation formulas were summarized and investigated. Then, they were analyzed, demonstrated, and discussed for testing with square wave signal only. After that, the symmetric formulas were approached into two types, such as the HIST interpolation and the LOST interpolation. The combination of the Forward and Backward operations was used to formulate the above methods. The typical synthetic signals, i.e., square wave, saw-tooth wave, and sine wave signals, were applied to evaluate the interpolation performance. Three conventional interpolation methods, i.e., nearest neighbor interpolation, linear interpolation, and cubic spline interpolation were employed for comparing the proposed method performance with the PSNR indicator. The simulation results show that the HIST interpolation has a high sensitivity to the data change. In contrast, the LOST interpolation gives a low sensitivity to the data change. The LOST interpolation gives the PSNR value, for all tested resolutions, higher than others, except for the sine wave signal that is lower than the cubic spline interpolation. However, the vision results show that it has a small difference. The option number increasing provides higher sensitivity than the lower value. Moreover, both our proposed symmetric methods also give the tilt behavior, which is dependent on the slope of sample data for both sides of the interpolation interval. Finally, both our symmetric interpolations still converge to the steady-state faster than the cubic spline interpolation.

REFERENCES

- [1] W. Mu, M. G. Amin, and Y. Zhang, "Bilinear signal synthesis in array processing," *IEEE Transactions on Signal Processing*, vol. 51, no. 1, pp. 90–100, Jan. 2003, doi: 10.1109/TSP.2002.806577.
- [2] S. Khetkeeree and C. Chansamorn, "Signal reconstruction using second order tetration polynomial," in *34th International Technical Conference on Circuits/Systems, Computers and Communications, ITC-CSCC 2019*, Jun. 2019, pp. 1–4, doi: 10.1109/ITC-CSCC.2019.8793435.
- [3] S. V. Porshnev, D. V. Kusaykin, and M. A. Klevakin, "On accuracy of periodic discrete finite-length signal reconstruction by means of a Whittaker-Kotelnikov-Shannon interpolation formula," in *Proceedings - 2018 Ural Symposium on Biomedical Engineering, Radioelectronics and Information Technology, USBEREIT 2018*, May 2018, pp. 165–168, doi: 10.1109/USBEREIT.2018.8384577.
- [4] S. Luo, G. Bi, T. Wu, Y. Xiao, and R. Lin, "An effective LFM signal reconstruction method for signal denoising," *Journal of Circuits, Systems and Computers*, vol. 27, no. 9, Aug. 2018, Art. no. 1850140, doi: 10.1142/S0218126618501402.
- [5] N. MOHD NAWI, "Enhancing knowledge hyper surface method for casting diagnosing," *IAES International Journal of Artificial Intelligence (IJ-AI)*, vol. 2, no. 1, Mar. 2013, doi: 10.11591/ij-ai.v2i1.584.
- [6] H. Prasetyo, C. H. Hsia, and B. A. P. Akardihas, "Halftoning-based BTC image reconstruction using patch processing with border constraint," *Telkonnika (Telecommunication Computing Electronics and Control)*, vol. 18, no. 1, pp. 394–406, Feb. 2020, doi: 10.12928/TELKOMNIKA.v18i1.12837.
- [7] A. R. A. Nazren, R. Ngadiran, and S. N. Yaakob, "Edge enhancement of IBP reconstruction by using sharp infinite symmetrical exponential filter," *Indonesian Journal of Electrical Engineering and Computer Science (IJECS)*, vol. 14, no. 1, pp. 258–266, Apr. 2019, doi: 10.11591/ijeecs.v14.i1.pp258-266.
- [8] P. T. Tin, M. Tran, L. A. Vu, N. Q. Dung, and T. T. Trang, "Real interpolation method for transfer function approximation of distributed parameter system," *Telkonnika (Telecommunication Computing Electronics and Control)*, vol. 17, no. 4, pp. 1941–1947, Aug. 2019, doi: 10.12928/TELKOMNIKA.V17I4.11088.
- [9] P. T. Tin, T. H. Q. Minh, T. T. Trang, and N. Q. Dung, "Using real interpolation method for adaptive identification of nonlinear inverted pendulum system," *International Journal of Electrical and Computer Engineering (IJECE)*, vol. 9, no. 2, pp. 1078–1089, Apr. 2019, doi: 10.11591/ijece.v9i2.pp1078-1089.
- [10] K. A. Sai and K. Ravi, "An efficient filtering technique for denoising colour images," *International Journal of Electrical and Computer Engineering (IJECE)*, vol. 8, no. 5, pp. 3604–3608, Oct. 2018, doi: 10.11591/ijece.v8i5.pp3604-3608.
- [11] C. H. Hsieh, S. Y. Hung, C. W. Lan, and P. C. Huang, "Impulse noise removal based on grey polynomial interpolation," in *ITNG2010 - 7th International Conference on Information Technology: New Generations*, 2010, pp. 327–331, doi: 10.1109/ITNG.2010.38.
- [12] V. Patanavijit, "Denoising performance analysis of adaptive decision based inverse distance weighted interpolation (DBIDWI) algorithm for salt and pepper noise," *Indonesian Journal of Electrical Engineering and Computer Science (IJECS)*, vol. 15, no. 2, pp. 804–813, Aug. 2019, doi: 10.11591/ijeecs.v15.i2.pp804-813.
- [13] P. Thanakitvivil, S. Khetkeeree, C. Chansamorn, and C. Chansamorn, "Using High Boost Bi-cubic Interpolation to Upscale and Enhance the Medical Image Details," in *17th International Conference on Electrical Engineering/Electronics, Computer, Telecommunications and Information Technology, ECTI-CON 2020*, Jun. 2020, pp. 702–705, doi: 10.1109/ECTI-CON49241.2020.9158079.
- [14] J. Na'am, J. Santony, Y. Yuhandri, S. Sumijan, and G. W. Nurcahyo, "Enlarge medical image using line-column interpolation (LCI) method," *International Journal of Electrical and Computer Engineering (IJECE)*, vol. 8, no. 5, pp. 3620–3626, Dec. 2018, doi: 10.11591/ijece.v8i5.pp3620-3626.
- [15] H. Takeda and P. Milanfar, "An adaptive nonparametric approach to restoration and interpolation for medical imaging," in *Proceedings - 2009 IEEE International Symposium on Biomedical Imaging: From Nano to Macro, ISBI 2009*, Jun. 2009, pp. 666–669, doi: 10.1109/ISBI.2009.5193135.
- [16] T. M. Lehmann, C. Gönner, and K. Spitzer, "Addendum: B-spline interpolation in medical image processing," *IEEE Transactions on Medical Imaging*, vol. 20, no. 7, pp. 660–665, Jul. 2001, doi: 10.1109/42.932749.
- [17] H. Guedri, M. Ben Abdallah, and H. Belmabrouk, "Modelization using the B-spline method of blood vessel curve for the human retina," in *2017 International Conference on Control, Automation and Diagnosis, ICCAD 2017*, Jan. 2017, pp. 411–415, doi: 10.1109/CADIAG.2017.8075694.
- [18] A. Al-Mnayyis, S. A. Alasal, M. Alsmirat, Q. B. Baker, and S. Al Zu'bi, "Lumbar disk 3D modeling from limited number of MRI axial slices," *International Journal of Electrical and Computer Engineering (IJECE)*, vol. 10, no. 4, pp. 4101–4108, Aug. 2020, doi: 10.11591/ijece.v10i4.pp4101-4108.
- [19] H. Kim, Y. Cha, and S. Kim, "Curvature interpolation method for image zooming," *IEEE Transactions on Image Processing*, vol. 20, no. 7, pp. 1895–1903, Jul. 2011, doi: 10.1109/TIP.2011.2107523.
- [20] Jiazheng Shi and S. E. Reichenbach, "Image interpolation by two-dimensional parametric cubic convolution," *IEEE Transactions on Image Processing*, vol. 15, no. 7, pp. 1857–1870, Jul. 2006, doi: 10.1109/TIP.2006.873429.
- [21] R. G. Keys, "Cubic Convolution Interpolation for Digital Image Processing," *IEEE Transactions on Acoustics, Speech, and Signal Processing*, vol. 29, no. 6, pp. 1153–1160, Dec. 1981, doi: 10.1109/TASSP.1981.1163711.
- [22] A. Singh and J. Singh, "Content adaptive single image interpolation based Super Resolution of compressed images," *International Journal of Electrical and Computer Engineering (IJECE)*, vol. 10, no. 3, pp. 3014–3021, Jun. 2020, doi: 10.11591/ijece.v10i3.pp3014-3021.
- [23] Q. Wang and R. K. Ward, "A new orientation-adaptive interpolation method," *IEEE Transactions on Image Processing*, vol. 16, no. 4, pp. 889–900, Apr. 2007, doi: 10.1109/TIP.2007.891794.
- [24] J. S. Choi and M. Kim, "Super-interpolation with edge-orientation-based mapping kernels for low complex 2× upscaling," *IEEE Transactions on Image Processing*, vol. 25, no. 1, pp. 469–483, Jan. 2016, doi: 10.1109/TIP.2015.2507402.
- [25] K. Y. Li, W. D. Wang, K. W. Zheng, W. B. Liu, and G. L. Xu, "The application of B-spline based interpolation in real-time image enlarging processing," in *2014 2nd International Conference on Systems and Informatics, ICSAI 2014*, Nov. 2015, pp. 823–827, doi: 10.1109/ICSAI.2014.7009398.
- [26] L. Ji, R. Zhang, H. Han, and A. Chaddad, "Image magnification based on bicubic approximation with edge as constraint," *Applied Sciences (Switzerland)*, vol. 10, no. 5, Mar. 2020, doi: 10.3390/app10051865.
- [27] C. Deng, J. Liu, W. Tian, S. Wang, H. Zhu, and S. Zhang, "Image super-resolution reconstruction based on L1/2 Sparsity," *Bulletin of Electrical Engineering and Informatics*, vol. 3, no. 3, Sep. 2014, doi: 10.12928/eei.v3i3.284.
- [28] M. Abed Uthaib and M. Sadik Croock, "Vehicle plate localization and extraction based on hough transform and bilinear

- operations,” *Indonesian Journal of Electrical Engineering and Computer Science (IJECS)*, vol. 20, no. 2, pp. 1088–1097, Nov. 2020, doi: 10.11591/ijeecs.v20.i2.pp1088-1097.
- [29] H. Nguyen-Quoc and V. Truong Hoang, “Rice seed image classification based on HOG descriptor with missing values imputation,” *TELKOMNIKA (Telecommunication Computing Electronics and Control)*, vol. 18, no. 4, pp. 1897–1903, Aug. 2020, doi: 10.12928/telkomnika.v18i4.14069.
- [30] Y. Biadgie, “Near-lossless image compression using an improved edge adaptive hierarchical interpolation,” *Indonesian Journal of Electrical Engineering and Computer Science (IJECS)*, vol. 20, no. 3, pp. 1576–1583, Dec. 2020, doi: 10.11591/ijeecs.v20.i3.pp1576-1583.
- [31] C. Periyasamy, “Satellite image enhancement using dual tree complex wavelet transform,” *Bulletin of Electrical Engineering and Informatics (BEEI)*, vol. 6, no. 4, pp. 334–336, Dec. 2017, doi: 10.11591/eei.v6i4.861.
- [32] C. K. Yang, F. P. Shan, and T. L. Tien, “Climate change detection in penang island using deterministic interpolation methods,” *Indonesian Journal of Electrical Engineering and Computer Science (IJECS)*, vol. 19, no. 1, pp. 412–419, Jul. 2020, doi: 10.11591/ijeecs.v19.i1.pp412-419.
- [33] Q. N. Tran and S. H. Yang, “Efficient video frame interpolation using generative adversarial networks,” *Applied Sciences (Switzerland)*, vol. 10, no. 18, Sep. 2020, doi: 10.3390/AP10186245.
- [34] M. K. Hadi, “Utilization of the finite element method for the calculation and examination of underground power cable ampacity,” *International Journal of Applied Power Engineering (IJAPE)*, vol. 8, no. 3, Dec. 2019, Art. no. 257, doi: 10.11591/ijape.v8.i3.pp257-264.
- [35] Y. A. Akter, M. A. Rahman, and M. O. Rahman, “Quantitative analysis of Mouza map image to estimate land area using zooming and Canny edge detection,” *Telkomnika (Telecommunication Computing Electronics and Control)*, vol. 18, no. 6, pp. 3293–3302, Dec. 2020, doi: 10.12928/TELKOMNIKA.v18i6.16179.
- [36] Z. Qu, Y. Yang, and R. Wang, “Linear interpolation with edge-preserving adaptive weights,” in *Proceedings of the 2013 6th International Congress on Image and Signal Processing, CISP 2013*, Dec. 2013, vol. 1, pp. 506–510, doi: 10.1109/CISP.2013.6744048.
- [37] R. L. Goodstein, “Transfinite ordinals in recursive number theory,” *Journal of Symbolic Logic*, vol. 12, no. 4, pp. 123–129, Dec. 1947, doi: 10.2307/2266486.
- [38] D. E. Knuth, “Mathematics and computer science: Coping with finiteness,” *Science*, vol. 194, no. 4271, Dec. 1976, Art. no. 1235, doi: 10.1126/science.194.4271.1235.
- [39] M. H. Hooshmand, “Ultra power and ultra exponential functions,” *Integral Transforms and Special Functions*, vol. 17, no. 8, pp. 549–558, Aug. 2006, doi: 10.1080/10652460500422247.
- [40] N. Bromer, “Superexponentiation,” *Mathematics Magazine*, vol. 60, no. 3, pp. 169–174, Jun. 1987, doi: 10.1080/0025570X.1987.11977296.
- [41] J. Macdonnell, “Some critical points on the hyperpower function $x^{x^{x^{\dots}}}$,” *International Journal of Mathematical Education in Science and Technology*, vol. 20, no. 2, pp. 297–305, Mar. 1989, doi: 10.1080/0020739890200210.
- [42] I. Furuya and T. Kida, “Compaction of church numerals for higher-order compression,” in *Data Compression Conference Proceedings*, Mar. 2018, vol. 2018-March, Art. no. 408, doi: 10.1109/DCC.2018.00061.

BIOGRAPHIES OF AUTHORS



Chapkit Charnsamorn     received the B.Sc. degree in Applied Physics (Hons. II) from King Mongkut’s Institute of Technology Ladkrabang, Thailand, in 1991, and the M.Sc. degree in Mathematics from Ramkhamhaeng University, Thailand, in 2012. He has been working as a Senior Lecturer at Physics department, Mahanakorn University of Technology, Thailand since 1991. He can be contacted at email: chapkit@mut.ac.th.



Suphongs Khetkeeree     received the B.Sc. degree in Physics from Burapha University, Thailand, in 2003, the M.Sc. degree in Physics from Kasetsart University, Thailand, in 2007, and the Ph.D. degree in Electrical Engineering from Mahanakorn University of Technology, Thailand, in 2018. He has been working as a Lecturer at Physics department, Mahankorn University of Technology, Thailand, since 2007. His research interests include signal and image reconstruction and remote sensing applications. He can be contacted at email: suphongs@mutacth.com.